Martín-Cabezuelo, R.; Vilariño, G.; Vallés Lluch, A. (2021). Influence of pre-polymerisation atmosphere on the properties of pre- and poly(glycerol sebacate). Materials Science and Engineering C. 119:1-10. https://doi.org/10.1016/j.msec.2020.111429

INFLUENCE OF PRE-POLYMERISATION ATMOSPHERE ON THE PROPERTIES OF PRE- AND POLY(GLYCEROL SEBACATE)

Rubén Martín-Cabezuelo[1], Guillermo Vilariño-Feltrer[1], Ana Vallés-Lluch[1,2,*]

[1] Centre for Biomaterials and Tissue Engineering, Universitat Politècnica de València, Spain

[2] Biomedical Research Networking Centre in Bioengineering, Biomaterials and Nanomedicine (CIBER-BBN), Valencia, Spain

[*] Correspondence: avalles@ter.upv.es

FOR TABLE OF CONTENTS USE ONLY

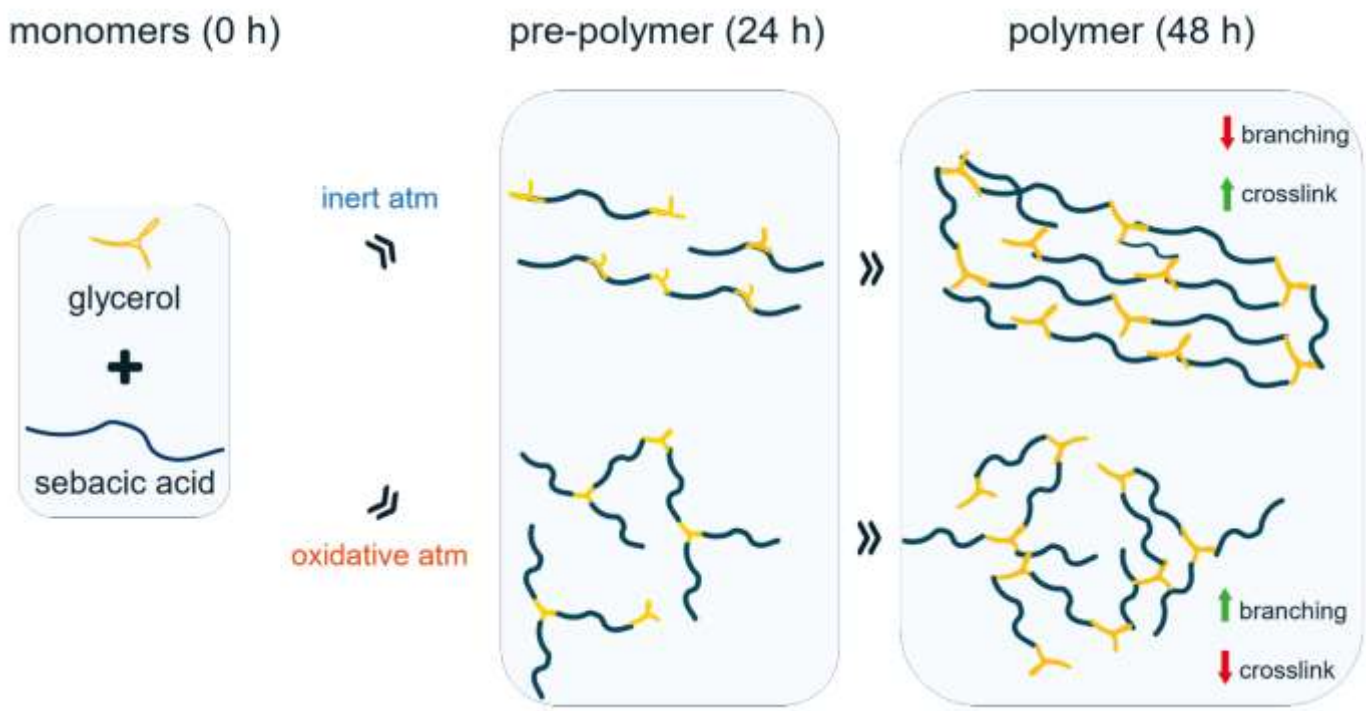

INFLUENCE OF PRE-POLYMERISATION ATMOSPHERE ON THE PROPERTIES OF PRE- AND POLY(GLYCEROL SEBACATE)

Rubén Martín-Cabezuelo[1], Guillermo Vilariño-Feltrer[1], Ana Vallés-Lluch[1,2,*]

[1] Centre for Biomaterials and Tissue Engineering, Universitat Politècnica de València, Spain

[2] Biomedical Research Networking Centre in Bioengineering, Biomaterials and Nanomedicine (CIBER-BBN), Valencia, Spain

[*] Correspondence: avalles@ter.upv.es

ABSTRACT

Poly(glycerol sebacate) (PGS) is a versatile biodegradable biomaterial on account of its adjustable mechanical properties as an elastomeric polyester. Nevertheless, it has shown dissimilar results when synthesised by different research groups under equivalent synthesis conditions. This lack of reproducibility proves how crucial it is to understand the effect of the parameters involved on its manufacturing and characterise the polymer networks obtained. Several studies have been conducted in recent years to understand the role of temperature, time, and the molar ratio of its monomers, while the influence of the atmosphere applied during its pre-polymerisation remained unknown. The results obtained here allow for a better understanding about the effect of inert (Ar and N_2) and oxidative (oxygen, dry air, and humid air) atmospheres on the extent of the reaction. The molecular pattern of intermediate pre-polymers and the gelation time and morphology of their corresponding cured PGS networks were studied as well. Overall, inert atmospheres promote a rather linear growth of macromers, with scarce branches, resulting in loose elastomers with long chains mainly crosslinked. Conversely, oxygen in the latter atmospheres promotes branching through secondary hydroxyl groups, leading to less-crosslinked 'defective' networks. In this way, the pre-polymerisation atmosphere could be used advantageously to adjust the reactivity of secondary hydroxyls, in order to modulate branching in the elastomeric PGS networks obtained to suit the properties required in a particular application.

Keywords: poly(glycerol sebacate); polymerisation atmosphere; glycerol; polycondensation; pre-polymerisation; curing

1. INTRODUCTION

Poly(glycerol sebacate) (PGS) is an elastomeric polyester with suitable properties for biomedical and tissue engineering applications, such as biodegradability and biocompatibility [1–4]. First reported as a biomaterial by Wang *et al.* in 2002 [5], PGS can be manufactured in a wide range of consistencies, from soft to hard [6], enhancing tissue regeneration and/or substitution [3]. Its versatility enables mimicking the mechanical and structural features of several tissues, such as cornea [7,8], adipose [9], blood, cartilage, nerve [10], cardiac muscle [11,12] and bone [13–15]. Additionally, modifications have recently been done in various ways to overcome its limitations and broaden its applications. Examples include: copolymerization with aniline trimer [16] or pentamer [17] to confer electroactivity to the elastomers, a modular approach to obtain photopolymerizable methacrylated poly(ethylene glycol)-co-poly(glycerol sebacate) multi-block

copolymers [18], blending the PGS pre-polymer with poly(vinyl alcohol) to overcome solubility/melting drawbacks [19], blending PGS with poly(L-lactic acid) to enhance scaffold cell penetration and tissue in-growth [9], grafting it with ureido-pyrimidinone [20] to obtain supramolecular elastomers with self-healing and shape-memory properties, or adding silica glass [21] to confer bioactivity for bone tissue regeneration applications.

PGS synthesis is typically based on a two-stage polycondensation, starting with the pre-polymerisation of its reagents glycerol (Gly) and sebacic acid (SA). Carboxylic groups of the diacid condense with hydroxyl groups of the triol leading to ester groups (and a water molecule), eventually yielding oligo- or macromers, most of which are presumably linear, while they might be branched due to the tri-functionality of the alcohol. This pre-polymerisation process is conventionally carried out at constant temperature around 120 ºC-130 ºC, for 24 h under an inert atmosphere such as nitrogen or argon to prevent oxidation of reagents [5,22]. The pre-polymer (pPGS) is a wax-like mixture of species that can still be dissolved. The different species eventually start curing into a solid elastomer, when the condensation of terminal groups of branched chains causes the gelation of a percolated network. This second stage of the process goes on typically for 48 h under vacuum conditions at the same temperature, leading to a flexible polymer (PGS) [15,23-28].

In the last two decades, some studies have revealed the need for an optimised, simple and reproducible synthesis procedure, to avoid variability in the final properties of the polymer, and reduce manufacturing costs [23,29]. On the one hand, some authors have addressed the influence of synthesis parameters for a better understanding of the synthesis process and clarify how they alter the final polymer properties. Temperature stands as the most studied parameter during pre-polymerisation and curing of PGS, ranging between 110 ºC and 150 ºC [24,27]. Furthermore, curing time has also been investigated, as well as the ratio between monomers [29]. On the other hand, to further reduce the synthesis time, the use of a microwave oven has been proposed, for example. The drawback of this method is that the synthesis rate is faster at the expense of glycerol loss because of the high temperatures reached, thereby distorting the molar ratio between monomers [29,30]. Other authors performing a microwave-assisted synthesis showed that, by using a water-based reagent mixture, the reaction temperature remained more homogenous and kinetics decelerated. This is due to the fact that water is a by-product of the esterification between Gly and SA, thanks to the solvent diffusion effect, leading to a more reproducible reaction [31].

Notwithstanding the foregoing, the PGS synthesis is conventionally conducted under an inert atmosphere to replicate the condition set when it was synthesised for the first time by Nagata *et al.* in 1998 under the name of Yg10, using a nitrogen atmosphere [22]. Although the polymerisation temperatures are milder than those reported in this foremost work (215 ºC-250 ºC), no studies have reported to date the real need for an inert atmosphere, and its effect on the resulting viscous pre-polymer remains undetermined.

To unveil the potential influence of this parameter, pre-polymerisation was tested over 24 h at 130 ºC as described in [24], but in different atmosphere compositions. The environments selected were: argon (Ar) and nitrogen (N_2) as inert gases; oxygen (O_2), which may produce oxidative reactions due to its interaction with glycerol hydroxyls [32,33]; dry (compressed) air (DA), as a combination of inert and oxidative atmospheres; and humid air (HA) to study the additional effect of environmental water vapour. Next, the obtained pre-polymers were cured at 130 ºC for 48 h, to correlate properties of pPGS (and their corresponding PGS elastomer) with the synthesis atmosphere. However, vacuum was not applied at this stage, as is usually done, because it was previously [24] found to be not essential for crosslinking to occur (a mass fraction of 94% of effectively crosslinked chains was obtained after open-air curing of pre-polymers obtained under N_2, at 130 ºC for 48 h). This approach will enable monitoring the performance of pre-polymerisation as required, to then manipulate the viscous mixture and shape the cured PGS as a scaffold or porous membrane, for example, and set optimal the fabrication procedure.

Thus, PGS networks would be obtained matching the properties demanded by a particular biomedical application, either as loose elastomers with a high molecular weight between crosslinks or as branched, less crosslinked and softer ones.

2. MATERIALS AND METHODS

2.1. Preparation of pPGS pastes and PGS films

PGS pre-polymers (pPGS) were synthesised by condensation of glycerol (Gly; 99%, Sigma-Aldrich) and sebacic acid (SA; 99% Sigma-Aldrich), as reported in detail in a previous work [24]. An equimolar Gly:SA mixture (*i.e.* 3:2 ratio of OH:COOH functional groups) was heated up briefly to 140 ºC (above the SA melting point) to ensure homogeneity, and then kept at 130 ºC. The gas flow circulating through the reactor during pre-polymerisation was selected from N_2, Ar, O_2, dry air (DA) and humid air (HA; 33% relative humidity). The pre-polymerisation reaction was prolonged in each case to several time points up to 24 h. Next, the viscous pPGS was withdrawn and cured in Teflon® open-air moulds in a forced ventilation oven (Memmert UF160) at atmospheric pressure, at 130 ºC for 48 h, to obtain 1-mm thick PGS films.

After curing, the films were rinsed in tetrahydrofuran (THF, Scharlau) for two days in an orbital shaker with a solvent renewal, to remove unreacted monomer residues and non-crosslinked chains. Next, THF was progressively replaced with ethanol (EtOH; absolute ethanol, Scharlau) over two additional days to avoid the fracture of swollen networks, concluding with the gradual change to Ultra-pure MilliQ water for the last two days. Finally, PGS samples were dried overnight at room conditions, and then in a vacuum for 24 h. Unless otherwise specified, the films were cut into 6 mm diameter samples.

2.2. Characterization of pPGS pastes under different atmospheres

2.2.1. Degree of esterification of pPGSs

The degree of esterification (DE) of pPGSs obtained under each atmosphere after 24 h of synthesis was determined by titration method, adapted from [29]. The DE of the starting Gly:SA monomer mixture (mPGS) was also obtained for comparison. To this effect, 100 mg of viscous pPGS were poured into an Erlenmeyer flask with 50 mL of a 25:75% wt EtOH:THF solution and placed on a stirrer at 500 rpm until completely dissolved. Then, 5 drops of 0.5% phenol red solution (Sigma-Aldrich) were added for pH-monitoring, and the Erlenmeyer flask was sealed with parafilm to prevent atmospheric CO_2 to form K_2CO_3. A 0.1 M solution of potassium hydroxide (KOH; Sigma-Aldrich) in EtOH was added drop-by-drop to perform the titration, until the colour of the solution changed from transparent to pinkish-purple, indicating a pH value of 10.7. The final degree of esterification was calculated using the following equation, adapted from [29]:

$$DE = 1 - {(V_1 - V_0)}/{(V_{mon} - V_0)} \quad (1)$$

where V_1 is the volume of KOH solution used to titrate each pre-polymer sample, and V_0 and V_{mon} are the volumes used for the blank test and consumed by mPGS, respectively.

2.2.2. Fourier-Transform Infrared Spectroscopy

Fourier-Transform Infrared Spectroscopy (FTIR) spectra of pPGS samples obtained at different reaction time points up to 24 h were collected to follow the progress of hydroxyl, carboxylic and ester bonds under different synthesis atmospheres. A Platinum ATR spectrometer (ALPHA II, Bruker) was used for this purpose. The spectra resulted from averages of 24 scans at a resolution of 4 cm^{-1}, between 400 and 4000 cm^{-1}.

2.2.3. Differential Scanning Calorimetry measurements

Differential Scanning Calorimetry (DSC) measurements of pPGSs (pre-polymerised for 24 h) and mPGS were performed in a Perkin Elmer DSC 8000. Samples were cooled to -80 ºC, and scanned up to 60 ºC at 20 ºC·min^{-1} under a constant N_2 flow of 50 ml/min. The melting point was determined for each sample from its calorimetric curve as the maximum of the endothermic peak.

2.2.4. Thermogravimetric analysis

Thermal degradation tests of pPGS samples (polymerised for 24 h) were performed to

determine the effect of the atmosphere composition on the thermal decomposition profile of the pastes. A SDTQ600 thermogravimetric analyser (TGA, TA Instruments) was used to register the mass loss from 30 °C to 600 °C at a heating rate of 10 °C min^{-1} under a N_2 flow of 50 ml/min. The monomer mixture (mPGS) was measured for comparison.

2.3. Characterization of PGS cured after pre-polymerisation at different atmospheres

FTIR, TGA and DSC measurements were also performed on PGS samples as previously described. Additionally, the following experiments were conducted:

2.3.1. Viscosity tests

A Discovery HR-2 hybrid rheometer (TA Instruments) was used to scan the viscosity of pPGS samples during gelation until the rupture of the formed elastomer. pPGS pastes were placed between aluminium, 25 mm-diameter, parallel plates, separated by a gap of 1000 µm. The viscosity was recorded throughout the curing process at constant temperature (130 ºC) at 1.5 $rad \cdot s^{-1}$ of rotational speed.

2.3.2. Wettability tests

Dry PGS samples were analysed using a Dataphysics OCA 25 (DataPhysics Instruments GmbH), to determine their wettability. Water contact angles (WCAs) were obtained from at least ten 3 ul-drops of Ultra-pure MilliQ water for each sample, by the sessile drop technique. In order to unveil the presence of surface-hidden polar groups in the elastomers, as observed in [24], the WCAs of analogous wet samples were obtained. To this end, PGS samples were immersed for 24 h in Ultra-pure MilliQ water. The excess of water on the surfaces was carefully removed before measurements.

2.3.3. Swelling at equilibrium

An XS105 Dual Range balance (Mettler Toledo) was used for weighing dry PGS samples and later immersed in Ultra-pure MilliQ water at 37 ºC over different time lengths until constant weight. The equilibrium water content (EWC) was defined as follows:

$$EWC = {}^{m_w}/_{m} \quad (2)$$

where m_w is the mass of water in the swollen sample at equilibrium, and m is the mass of dry sample. In parallel, PGS networks were swollen in EtOH, a more affine solvent than water. These measurements might broaden differences between samples that remain subtle when swelling in water. An equation analogous to (2) was used to calculate the equilibrium EtOH content (EEC) in each case. Triplicate measurements were taken for each sample and solvent.

2.3.4. Density measurements

A Mettler ME 33360 density kit, accessory to the previously mentioned balance, was used to determine the density of dry PGS samples through Archimedes' principle. The samples were weighed open-air and immersed in n-octane (98 %, Sigma-Aldrich, $\rho_{\text{n-octane}}$ = 0.703 $g \cdot cm^{-3}$) at room temperature. It has been reported that PGS does not swell significantly in n-octane [24] and can thus be safely used in these tests. The density (ρ) was determined as the ratio of the weight of the dry sample (m) through the volume of n-octane displaced (V):

$$\rho = {}^{m}/_{v} = {}^{m}/_{(m\_\, m_{n-octane})/\rho_{n-octane}} \quad (3)$$

where $m_{n\text{-}octane}$ is the measured weight of the sample immersed in n-octane. Three samples were taken from every batch condition registered to carry out measurements.

2.3.5. Mechanical compression tests

In order to determine the compressive elastic modulus (E) of the PGS samples, a Thermomechanical Analysis device TMA/SS6000 Seiko Instruments Inc was used. Five replicates per PGS type were scanned. The experiments were conducted at room temperature between 0.5 and 1500 mN at 100 $mN \cdot min^{-1}$ to obtain the stress-strain curves. The elastic moduli were obtained from the slopes in the initial ramp, from 0 to 5 kPa, and in the second linear zone, in the range between 70 and 120 kPa.

2.3.6. Dynamic Mechanical Spectroscopy

Dynamic mechanical thermal analyses were performed to characterize the main relaxation process associated to the glass transition of PGS samples by means of a Dynamic Mechanical

Analyser DMA 8000 (PerkinElmer). Rectangular shaped specimens, approximately 100 mm^2, were tested from -80°C to 180°C at 3°C min^{-1} at 1 Hz of frequency in the single cantilever mode. The evolutions of the storage modulus (*E'*) and *tan* δ (the ratio between loss and storage moduli of viscoelastic materials) with temperature were recorded. To compare the different PGS samples, the temperature at the *tan* δ peak was determined.

3. RESULTS AND DISCUSSION

3.1. Influence of the pre-polymerisation atmosphere on the pPGS degree of esterification

In order to identify the chemical bonds and degree of esterification (DE) of pPGS viscous mixtures, FTIR and titration techniques were used. The FTIR spectra (Figure 1a) of all pPGS, mPGS and SA show a main peak at 1731 cm^{-1} assigned to the C=O stretching vibrations. The alkane groups (C-H) of the polymer backbone appear as two characteristic sharp peaks at 2855 cm^{-1} and 2927 cm^{-1}. mPGS and SA peak also at 1682 cm^{-1} is representative of the carbonyl stretching of the free carboxylic acid groups (-COOH). The peaks at 1045 cm^{-1} and 1097 cm^{-1} are indicative of the co-existence of primary and secondary saturated alcohol groups (C-O and O-H stretching) and evolve differently, same as the broad, unspecific band around 3440 cm^{-1}.

Generally speaking, during the pre-polymerisation of PGS, Gly alcohol groups react with free carboxyl groups of SA by means of condensation reactions to form ester groups. Several interesting findings can be inferred from the comparison between the FTIR spectra of pPGS mixtures obtained under different atmospheric conditions (Ar, N_2, DA, O_2 and HA) and Gly, SA and the monomeric mixture. Initially, primary hydroxyl groups are twice more frequent than secondary groups in the precursor Gly, as expected (Figure 1b). This ratio decreases below 1 when the pre-polymerisation with SA takes place, for all atmospheres tested, which suggests that, in an early stage, PGS synthesis yields mainly linear structures because of the superior reactivity of primary hydroxyl groups of Gly.

Simultaneously, as shown in Figure 1a, the sharp peak at 1682 cm^{-1} (free -COOH groups) from SA and mPGS shifts to 1710 cm^{-1} and then to 1730 cm^{-1} at the time ester groups ($-COO^-$) are formed. A similar trend is found in the hydroxyl broad band: the increase in transmittance of this band shifting from 3300 cm^{-1} to 3580 cm^{-1} and its area becoming smaller are indicative of esterification taking place by consuming hydroxyl groups. The high $-COO^-$/-COOH (Figure 1c) and low -OH/$-COO^-$ (Figure 1a, between brackets) ratios observed after 24 h of pre-polymerisation when it is performed under HA suggest that this atmosphere allows this reaction to take place most efficiently. N_2 apparently has the opposite effect.

The DE values obtained from the titration experiments with the pPGS samples are shown in Figure 1d. An increasing trend is observed when oxidative atmospheres are used (DA and O_2) and water vapour is present in the environment (HA). DE values around 72.5% and 66.40% for N_2 and Ar, respectively, are indicative of a lower interaction between -OH and free -COOH groups during these pre-polymerisations. The DE values in oxidative atmospheres are higher than in inert environments, around 76%. It can be confirmed that synthesis under atmospheres containing O_2 increases the ratio of initiation of the reaction, which is in accordance with [34]. Taken together, the FTIR and titration results suggest that oxidative atmospheres enhance the pre-polymerisation rate. Water vapour, for its part, may hinder the evaporation reactant Gly (that it is well known to occur [29]), bringing this reaction to a higher extent.

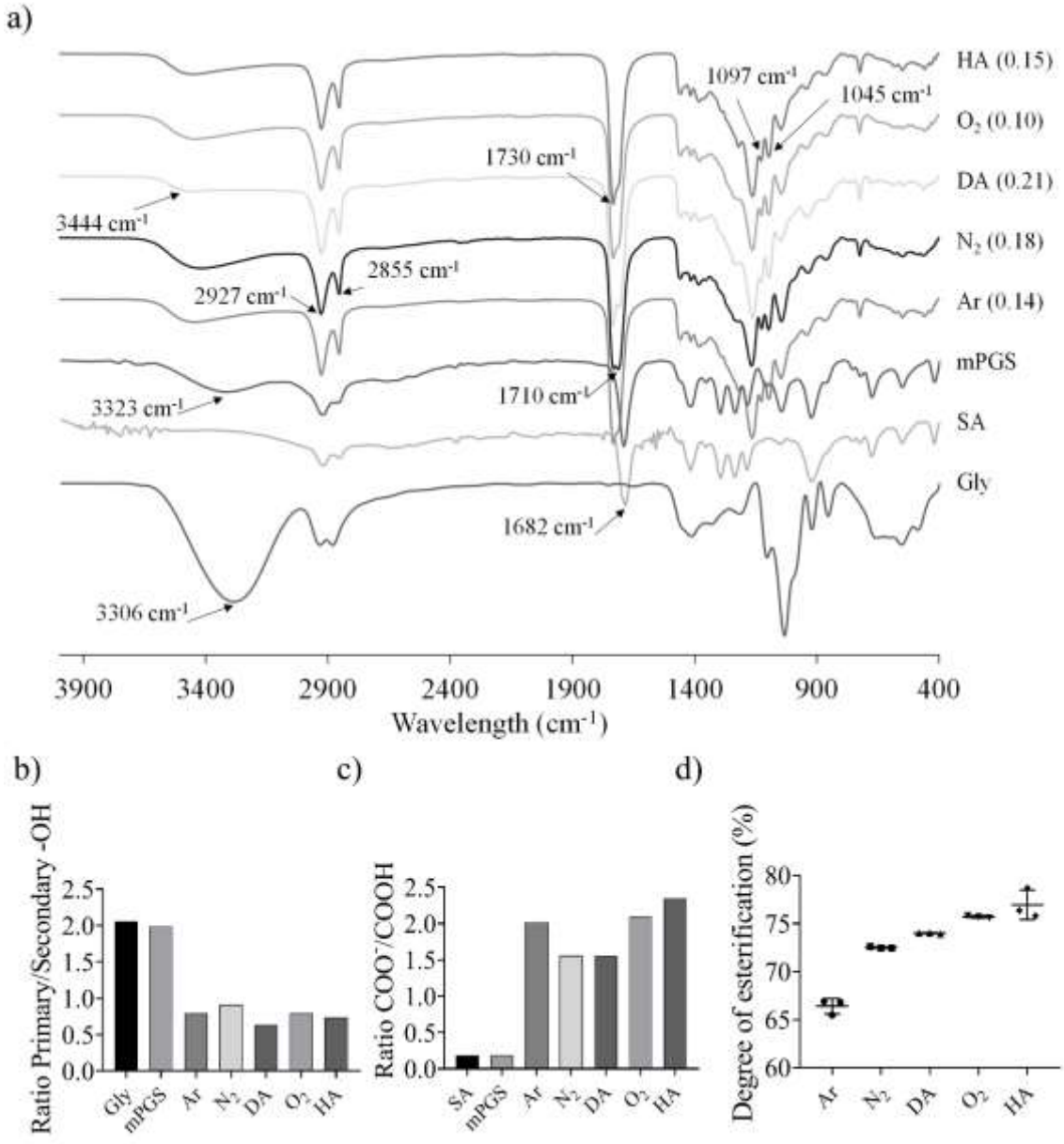

Figure 1. (a) FTIR spectra (transmittance) of pPGS mixtures pre-polymerised under different atmospheres for 24 h at 130 °C. The spectra of SA, Gly and mPGS mixture are represented as control values. The values between brackets show the transmittance ratio between 3480 cm^{-1} and 1730 cm^{-1} (-OH/-COO^-). (b) Ratio between primary and secondary hydroxyl groups obtained as the transmittance ratio between 1045 cm^{-1} and 1097 cm^{-1}. (c) Ratio between ester and free carboxylic acid obtained as the transmittance ratio between 1731 cm^{-1} and 1682 cm^{-1}, respectively. (d) Degree of esterification (DE) values of pPGS after pre-polymerisation under different atmospheres during 24 h at 130 ºC.

3.2. Influence of the pPGS degree of esterification on its thermal properties

Figure 2a shows the normalised power during the heating scan of the DSC measurements of pPGS samples, together with their melting point (T_m) values taken at the maximum of the melting endothermic peak. The monomers mixture displays two different T_m: one around 26 ºC (less intense), and another at 118.68 ºC (strong endothermic peak, shown in the insert at another scale), as expected given the different T_m of its constituents Gly (18.2 ºC) and SA (130.2 ºC). The melting peaks of the mixture unify as pre-polymerisation

occurs and the result gradually shifts to values around 10 ºC for inert atmospheres (12.24 ºC for Ar and 9.89 ºC for N_2) or lower when O_2 and/or environmental water are present (around 6 ºC for O_2 and HA samples). All these pre-polymers are, thus, still semicrystalline, whereas crosslinked PGS networks turned out to be fully amorphous after curing [24].

Although O_2 and HA have shown to esterify to a greater extent, the presence of oxidative species from Gly seems to facilitate chain mobility in the pPGS paste, lowering their T_m values. In the case of HA, diffusion of water vapour throughout the mixture taking place in the reactor could hinder the evaporation of Gly, as previously mentioned, thus acting synergistically with the oxidative ambient to this effect.

The thermogravimetric profiles of pPGSs and the monomer mixture are plotted in Figure 2b. For comparison purposes, the thermal degradation temperature has been tabulated at the inflection point of the main weight loss (T_d in the insert). Again, mPGS shows the behaviour of its components, with two weight loss stages, that of Gly (T_d = 213.93 ºC) and SA (T_d = 435.19 ºC). The pre-polymers display a mild weight loss between 175 and 275 ºC, attributed to free Gly (in excess in the monomer mixture), which is less evident as the reaction proceeds and it is further consumed, in oxidative environments. In accordance with this observation, T_d (calculated in the main weight loss stage, between 400 and 500 ºC) for pPGS obtained under Ar, N_2 and DA appears at around 425 ºC, while higher values are obtained under O_2 and HA atmospheres (428.59 ºC and 434.9 ºC, respectively).

Notwithstanding, it is worth mentioning that the profile of HA pPGS paste differs greatly from the rest, with a significant intermediate weight loss between 275 ºC and 400 ºC (around 20%), indicative of a wider variety of species in this pre-polymer, some more sensitive to thermal degradation.

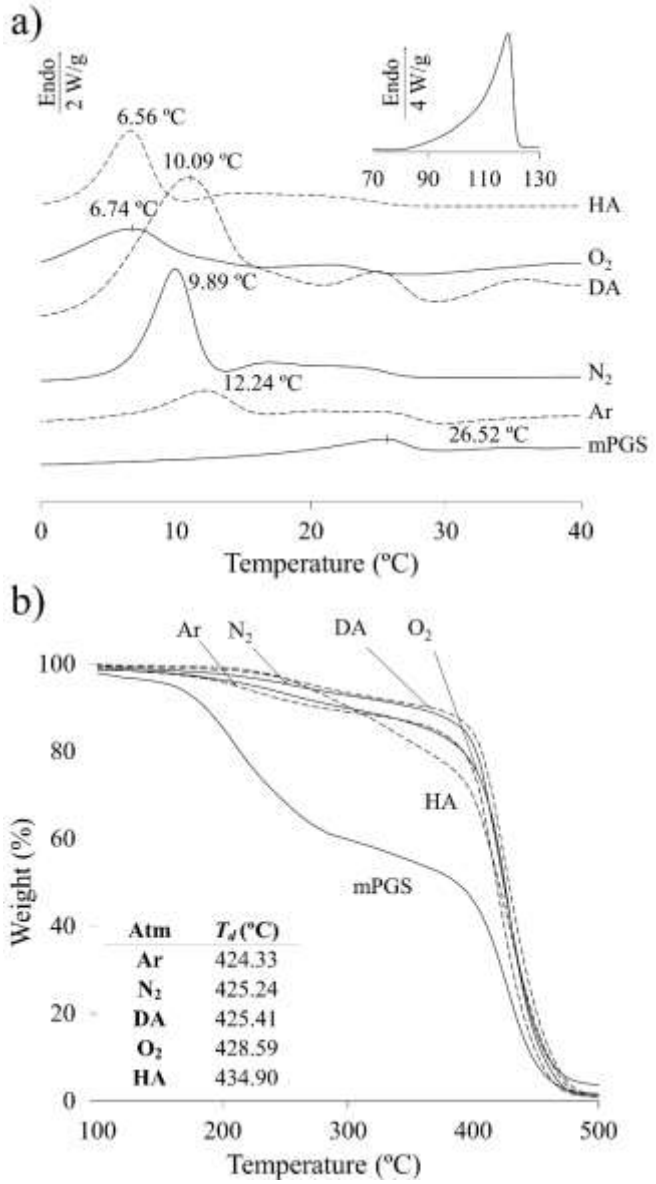

Figure 2. (a) DSC and (b) TGA thermograms plotting the normalised power and weight as a function of temperature, respectively, for mPGS and pPGS pastes obtained under different atmospheres after 24 h at 130 ºC. Values displayed in (a) are the melting temperatures (T_m) indicating the maximum value of the endothermic melting peak. The mPGS profile is shown as control, displaying in the insert the characteristic melting point of SA. Data in table on (b) lists the inflection point (T_d) of the main degradation stage, obtained from derivative curves.

3.3. Effect of the pre-polymerisation atmosphere on pPGS gelation

The viscosity rate over time was monitored simulating the curing step conditions of a PGS pre-polymer, in a force-ventilated oven at 130 ºC during 48 h as described in [24]. Gelation and subsequent polymerisation in the solid state

(curing) were monitored until the PGS networks broke under the stress exerted by the plates. The viscosity profiles of pPGS pastes, previously pre-polymerised (as polymer melt) under different atmospheric conditions, are presented in Figure 3. It is worth indicating that origin of x-axis (0 h) corresponds to the start of the second polymerisation stage, carried out in the rheometer. Table 1 lists the value of initial viscosity (η_0), gelation time (located at the intersection point of the extrapolated liquid and solid polymerisation trends), and the ultimate viscosity and time for it, obtained at the end of the experiment (breaking point). These results allow for a better understanding about the effect of each atmosphere on the resulting pPGS and the corresponding cured PGS network final morphology.

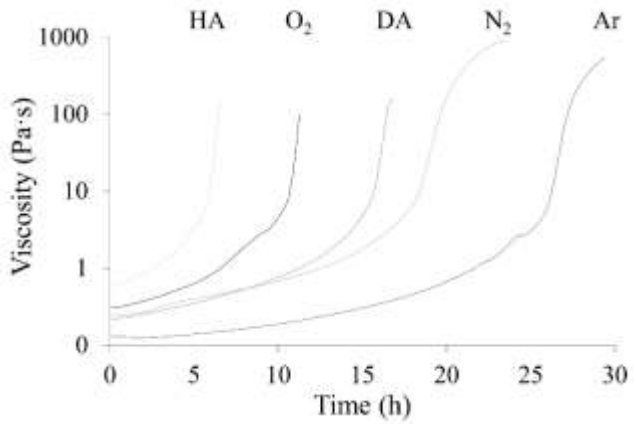

Figure 3. Viscosity monitoring of pPGS (pre-polymerised under different atmospheres) vs. time, at 130 ºC.

Initial viscosity values are higher for pastes obtained under HA, O_2 and DA atmospheres (higher degree of conversion at 0 h), which gel after few hours. This trend correlates with the amount of oxygen and water vapour in the tested environment. It has been proven that O_2 rich atmospheres applied during polymer synthesis may increase the viscosity of the solution, because of its high electron affinity which leads to an increase of reactivity by removing electrons from monomers [35]. In the case of HA, if one assumes that water vapour hinders the evaporation of Gly from the reacting mixture, as suggested before, its excess would enhance the formation of branched chains during the pre-polymerisation process, which explains its greater viscosity. Indeed, in [24] it was found that an excess of Gly in the reacting mixture promoted the activation of secondary hydroxyls and led (after pre-polymerisation under N_2 and curing) to highly-branched oligomers, poorly crosslinked to each other. Such samples lost, after rinsing, more than 70% of its weight, resulting in very sticky polymers, really difficult to handle. Besides, water has been found to thermally stabilize the reacting mixture by facilitating heat transfer [31], which could contribute to this effect. Inert atmospheres yield less viscous pastes that require longer times for the percolation of a crosslinked polymer, following a gradual and prolonged increase of viscosity. When compared, N_2 seems to favour the production of more viscous macromers (and probably slightly more branched) than Ar during the pre-polymerisation stage.

Table 1. Representative parameters of the curing process: initial (pPGS) viscosity (η_0), gelation time (t_{gel}), and ultimate (maximum, i.e. that of PGS) viscosity (η_{max}) attained in the rheometer at the breaking point (t_{max}) under the stress of its plates.

Atm	η_0 (Pa·s)	t_{gel} (h)	η_{max} (Pa·s)	t_{max} (h)
Ar	0.13	24.86	535.45	29.25
N_2	0.24	17.17	920.99	23.67
DA	0.22	15.08	155.66	16.92
O_2	0.31	10.25	96.63	11.33
HA	0.59	5.58	141.15	6.75

The final viscosity, obtained at the breaking point, correlates with the gelation time of the different pre-polymers: on those pre-polymerised under inert atmospheres the polymeric chains contribute more effectively to the elastomeric behaviour, while those obtained under oxidative atmospheres have a more branched morphology, being softer. All in all, the rheometry results point out that by setting the atmospheric conditions in the first polymerisation stage, not only the pre-polymers but also the PGS networks obtained greatly differ from each other.

3.4. Effect of the pre-polymerisation atmosphere on the physicochemical properties of cured PGS

The -OH/-COO^- ratio of PGS, obtained from their FTIR spectra (Figure 4a) does not differ significantly between samples, being close to 0.11 for all conditions. This indicates that the final cured PGS network achieves, insofar this experimental technique can provide chemical information about the polymeric matrix, equivalent endpoints following each pre-polymerisation atmosphere. If compared to Figure 1a, the pre-polymer obtained in presence of N_2 is, therefore, the resulting material with the lowest rate of terminal -OH during curing. As for the primary/secondary -OH ratio, it does not vary significantly during the curing process (Figure 4b), unlike during pre-polymerisation of mPGS (Figure 1b). Apparently, the consumption of primary hydroxyls is favoured, as opposed to secondary ones, during the whole process. Notwithstanding, networks pre-polymerised under oxidative atmospheres show slightly higher ratios, which agrees with branching through secondary hydroxyls described in the previous section. As for the ester/free carboxylic acid ratio (Figure 4c), it increased significantly from the values reached after pre-polymerisation (Figure 1c), especially for those obtained under inert atmospheres.

The density of the PGS networks, Figure 4d, slightly decreases after pre-polymerisation in oxidative and humid atmospheres. This finding, though subtle, supports the hypothesis that these conditions yield defective (less crosslinked) branched networks, and are aligned with the observations in [24,36] for PGS cured at mild temperatures.

The water contact angles of the surfaces are shown in Figure 4e, together with those obtained on wet analogous surfaces. The purpose of equilibrating the samples in water was to remove the potential effect of hydrogen-bonding interactions between polar terminal groups in the dry state, which has been observed in PGS samples [24] as in other rubbers [37], and better reveal differences in this respect. However, they are instead attenuated when hydrated. Still, they are evident between the DA and O_2 pre-polymers, being the least wettable, and the HA ones on the other extreme. An aspect worth noting is that oxygen in the reacting atmosphere presumably produces alcohol-oxidised species, namely aldehydes and/or carboxylic acids from primary hydroxyls or ketones from secondary ones, which slightly increase the wettability of these samples compared to those obtained under inert atmospheres. Indeed, up to eleven oxidation compounds of glycerol have been isolated and identified under distinct conditions (presence of salts, catalysts, free oxygen or sunlight, to name a few) [34].

Table 2. Equilibrium water (EWC) and EtOH (EEC) contents of cured PGS samples starting from different pPGS.

Atm	EWC (%)	EEC (%)
Ar	4.49 ± 1.36	86.60 ± 0.97
N_2	4.51 ± 1.89	91.14 ± 1.36
DA	4.99 ± 1.74	82.70 ± 3.31
O_2	5.70 ± 1.05	97.58 ± 3.69
HA	2.97 ± 1.53	84.69 ± 8.95

Although water is not as good as EtOH as a swelling solvent of PGS (20-fold higher content at equilibrium, according to Table 2), it can be argued that oxygen in the pre-polymerisation atmosphere slightly improves this feature in the resulting hydrophobic networks.

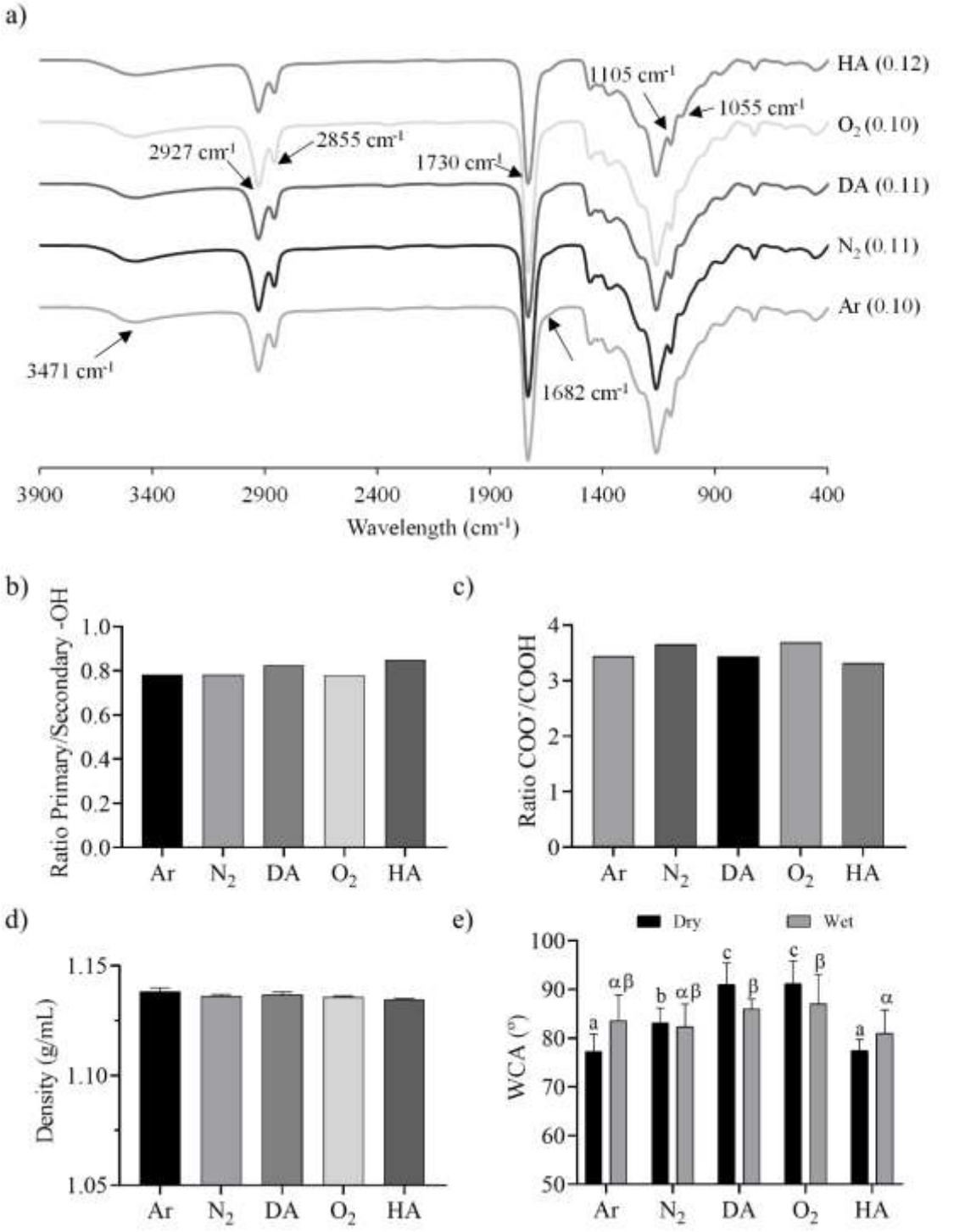

Figure 4. (a) FTIR spectra (transmittance, a.u.) of cured PGS networks previously pre-polymerised under different atmospheres. The values between brackets show the transmittance ratio between 3480 cm^{-1} and 1730 cm^{-1} (-OH/-COO^-). (b) Ratio between primary and secondary hydroxyl groups obtained as the transmittance ratio between 1045 cm^{-1} and 1097 cm^{-1}. (c) Ratio between ester and free carboxylic acid obtained as the transmittance ratio between 1731 cm^{-1} and 1682 cm^{-1}, respectively. (d) PGS density measurements. (e) Water contact angles (WCA) on cured samples, in their dry (black, Latin letters) state and after stabilisation in water (wet, grey, Greek letters). Sample data distributions were analysed through a one-way ANOVA and a post-hoc Games-Howell multiple mean comparison test, with a *p*-value of 0.05. Matching letters indicate homogeneous groups.

3.5. Effect of the pre-polymerisation atmosphere on thermal and mechanical properties of cured PGS

Figure 5a presents the normalised power in the DSC heating scan of PGS samples along with their melting points (T_m), when still detectable, and glass transition temperatures (T_g). The latter were located at the inflection point in the step of the baseline of the curves. The endothermic melting peaks vanish while the melting temperatures decrease compared to those of the pre-polymers and get closer to the glass transition. This effect is more evident for those samples pre-polymerised under the presence of oxygen, probably because branching hinders folding of polymer segments into crystallites. Indeed, in PGS pre-polymerised with HA, the melting peak of the crystalline phase is no longer discernible, which is characteristic of an amorphous elastomer. As for the glass transition temperatures, they range between -15 ºC to -25 ºC, being higher when crosslinking of macromers are more extensive and chain stiffness increases, *i.e.* under inert atmospheres.

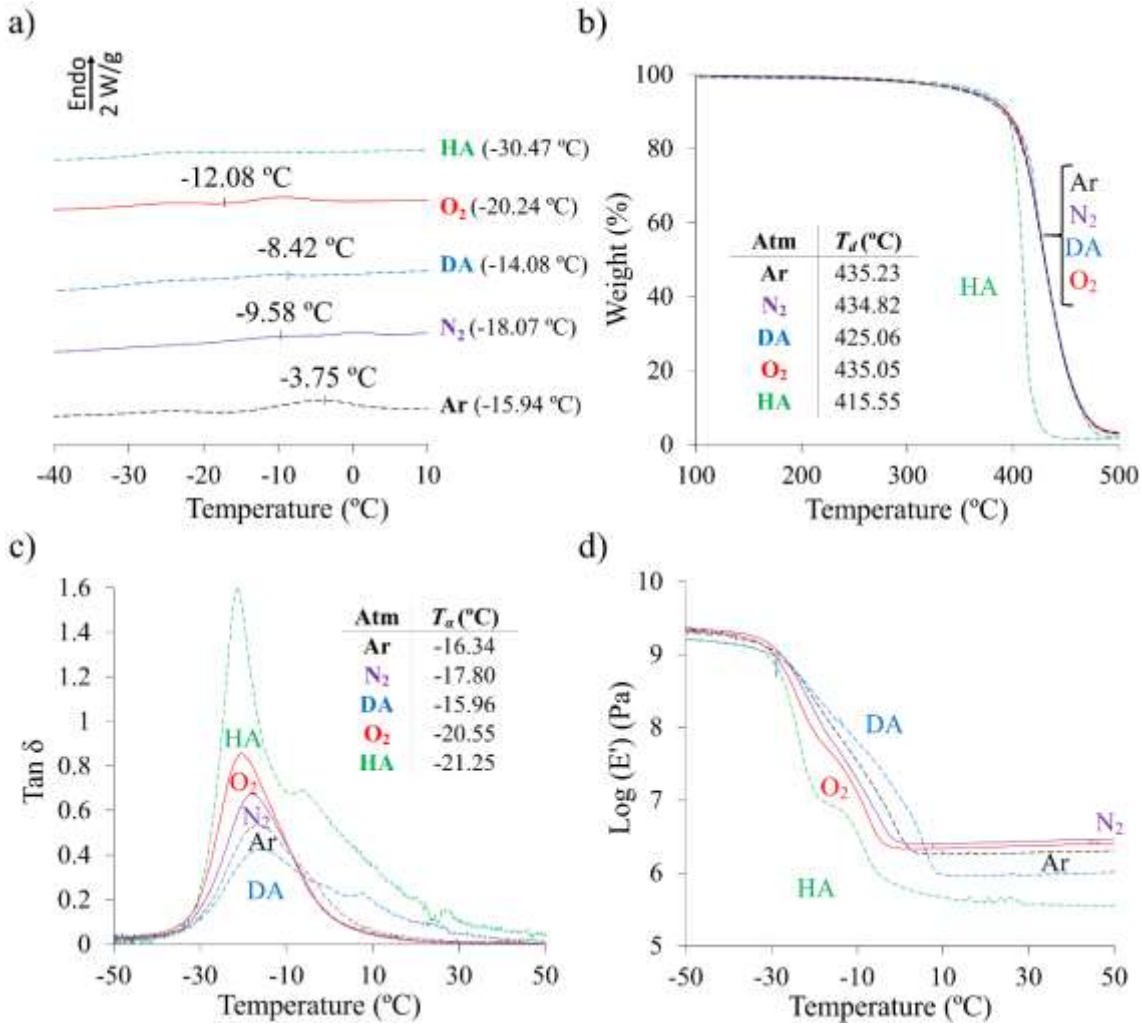

Figure 5. (a) DSC normalised power of PGS networks synthesised under different atmospheres, as a function of temperature. The melting temperatures (T_m) have been located at the maximum of the endothermic melting peak. Glass transition temperatures (T_g) between brackets. (b) TGA thermograms. Insert: inflection point (T_d) of the main degradation stage, obtained from derivative curves. (c) Temperature dependence of loss tangent ($tan\ \delta$) and (d) the storage moduli (E') of PGS networks pre-treated under different atmospheres. The insert in (c) lists the temperature of the maximum values of the main peak in $tan\ \delta$ (T_α) characterising the main relaxation process associated to the glass transition of PGS samples.

Weight loss curves from Figure 5b illustrate that PGS samples are stable up to 250 ºC, which coincides with the literature [38]. They show a single weight loss step in all cases, located between 350 ºC and 475 ºC, which overlaps in all samples except for HA PGS, which again shows weight loss at lower temperatures. This is, once more, indicative of its branched morphology, which, as observed during our monitorisation, leads to the presence of oligomers that decompose in the polymer matrix. Figures 5c and d, show the dynamic-mechanical spectra of the samples, in terms of the storage moduli (*E'*) and (b) loss tangent (*tan δ*).

The main relaxation appears between -30 ºC and 0 ºC for samples pre-polymerised under inert atmospheres and narrows to show an abrupt drop ending up at -20 ºC for those samples obtained under O_2 and HA. These results are consistent with the observations on the calorimetric profiles.

The temperature at the maximum of the associated peak in *tan δ*, T_α, shifts accordingly to lower temperatures, around -20 ºC. Interestingly, this peak displays a shoulder at higher temperatures, between -5 ºC and 10 ºC, for these samples, not so distinctively showing in the networks obtained under inert atmospheres. This indicates that the mobility of certain segments in these PGS networks is hindered up to these temperatures, probably due to branching that hinders rotations over the main chain bonds and decrease the flexibility of the polymer chain.

The stress-strain curves (Figure 6) of the PGS elastomers show the typical J-shaped behaviour of biological highly elastic soft tissues, displaying a "zero-stress" zone [39,40]. The compressive elastic moduli, E_1 and E_2, were taken at their two linear zones: the first slope from 0 to 5 KPa and the second from 70 to 120 KPa, and are listed in Table 3. The high-slope region ("high" modulus, E_2) can be attributed to tightening of primary, covalent bonds, whereas weak, secondary bonds, are overcome throughout the previous low-slope one (low modulus, E_1). E_1 values are of the order of those obtained in other works (253.41 kPa) [41]. Aligned with previous findings, these values are higher when networks are pre-polymerised under inert atmospheres. N_2, and even more Ar seem to promote a linear growing of macromers, with scarce branching, that eventually crosslink while curing. O_2 and water vapour in the atmosphere boost reactivity of secondary hydroxyls of Gly to react more readily, leading to more branched and eventually defective networks with lower mechanical properties. As for E_2, no trend is discernible. The values obtained are in all cases typical of elastomers, see [24] or [42] for comparison. In the former, Young's modulus was determined as the slope until 15% strain for PGS cured for varied temperatures and times, whereas in the latter, it was determined from the slope in the linear portion of the plot -< 20% strain- after tensile tests and varied 0.15-30 MPa for acrylated-PGS.

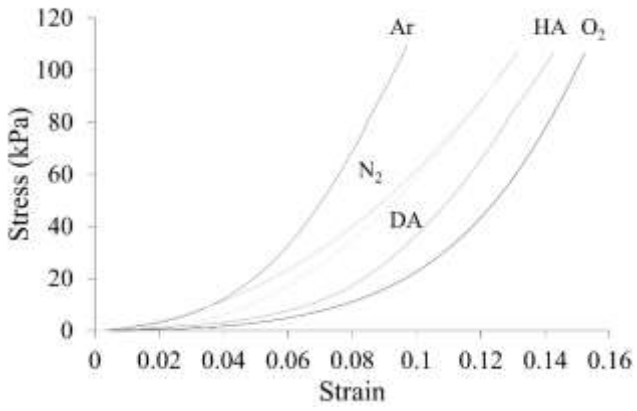

Figure 6. Stress-unitary strain average curves obtained from five compressive replicates of each PGS sample pre-treated under different atmospheres.

Table 3. Young moduli (*E*) evaluated in the two linear regions of the J-shaped compression curves, and bending modulus (E_{bend}), obtained as *E'* at 25 ºC from the DMS measurements.

Atm	E_1 (kPa)	E_2 (kPa)	E_{bend} (kPa)
Ar	380 ± 300	1750 ± 380	1859.7
N_2	230 ± 80	1580 ± 360	2650.6
DA	170 ± 100	1920 ± 430	951.8
O_2	110 ± 60	2470 ± 490	2299.9
HA	230 ± 150	1690 ± 130	434.4

The bending (or flexural) modulus, E_{bend}, obtained as *E'* at 25 ºC from Figure 5d, is also listed in Table 3. As occurred with E_2, E_{bend} does not reveal any

clear tendency, probably because the effect of crosslinks increasing it for samples pre-polymerized under inert atmospheres is disguised with that of bulky branchings when pre-polymerization is undergone under oxidative ones, which provokes, in turn, the secondary peak in *tan* δ.

4. CONCLUSIONS

It is widely accepted that PGS synthesis by condensation yields mainly linear structures in an early stage, because of the enhanced reactivity of primary hydroxyl groups of glycerol. Indeed, secondary hydroxyl groups appear to remain less reactive until primary -OH have been partially consumed. This work has shown that this can be easily strengthened, if it is of interest, by the synthesis atmosphere, leading to PGS networks with significantly different properties.

Thus, the results here presented reveal that, in the outlining of a PGS network, temperature, time, or the ratio between reactants Gly:SA aren't the only crucial variables to be taken into consideration, as it was previously considered, but also the reacting atmosphere during polymerisation in the liquid state, before gelation.

This so-called pre-polymerisation proceeds at a greater extent if carried out under oxidative atmospheres (DA, O_2 and HA), but in a branched fashion because of the simultaneous formation of oxidised species that boost the reactivity of secondary hydroxyls from Gly. Water vapour contributes to this effect, likely by hindering glycerol evaporation from the reacting mixture. Inert atmospheres, on the other hand (Ar even more than N_2), promote a rather linear growth of macromers, with scarce branching.

The pre-polymers obtained under inert atmospheres are less viscous. Nonetheless, the presence of glycerol and by-products thereof decrease the melting point of pastes obtained under oxidative and humid environments, which can also be an interesting feature when manufacturing PGS-based structures. The increase in viscosity is more gradual in pPGS obtained under inert atmospheres, thus gelation takes longer. The resulting networks are loose elastomers with long chains, overall effectively crosslinked. Conversely, the branched, less-crosslinked networks obtained after curing pre-polymers obtained in the presence of oxygen are less elastic and softer, and their main mechanical relaxation splits, as branching prevents the free rotation of the main chain.

Each of these pre-polymers, having singular properties and yielding different polymer morphologies, could find particular applications as biomaterials, particularly when processed to obtain microporous structures in the tissue engineering field.

5. ACKNOWLEDGMENTS

The assistance and advice of the Electron Microscopy Service of the Universitat Politècnica de València (Spain) is acknowledged.

6. DATA AVAILABILITY

The raw/processed data required to reproduce these findings cannot be shared at this time due to technical or time limitations.

7. REFERENCES

[1] Y. Wang, Y.M. Kim, R. Langer, In vivo degradation characteristics of poly(glycerol sebacate), J. Biomed. Mater. Res. 66A (2003) 192–197. https://doi.org/10.1002/jbm.a.10534.

[2] R. Rai, M. Tallawi, A. Grigore, A.R. Boccaccini, Synthesis, properties and biomedical applications of poly(glycerol sebacate) (PGS): A review, Prog. Polym. Sci. 37 (2012) 1051–1078. https://doi.org/10.1016/j.progpolymsci.2012.02.001.

[3] I. Manavitehrani, A. Fathi, H. Badr, S. Daly, A. Negahi Shirazi, F. Dehghani, Biomedical Applications of Biodegradable Polyesters, Polymers (Basel). 8 (2016) 20. https://doi.org/10.3390/polym8010020.

[4] P. Shirazaki, J. Varshosaz, A. Kharazi, Electrospun Gelatin/poly(Glycerol Sebacate) Membrane with Controlled Release of Antibiotics for Wound Dressing, Adv. Biomed. Res. 6 (2017) 105. https://doi.org/10.4103/abr.abr_197_16.

[5] Y. Wang, G.A. Ameer, B.J. Sheppard, R. Langer, A tough biodegradable elastomer, Nat. Biotechnol. 20 (2002) 602–606. https://doi.org/10.1038/nbt0602-602.

[6] B.D. Ulery, L.S. Nair, C.T. Laurencin, Biomedical applications of biodegradable polymers, J. Polym. Sci. Part B Polym. Phys. 49 (2011) 832–864. https://doi.org/10.1002/polb.22259.

[7] P. Stafiej, F. Küng, D. Thieme, M. Czugala, F.E. Kruse, D.W. Schubert, T.A. Fuchsluger, Adhesion and metabolic activity of human corneal cells on PCL based nanofiber matrices, Mater. Sci. Eng. C. 71 (2017) 764–770. https://doi.org/10.1016/j.msec.2016.10.058.

[8] S. Salehi, M. Fathi, S. Javanmard, F. Barneh, M. Moshayedi, Fabrication and characterization of biodegradable polymeric films as a corneal stroma substitute, Adv. Biomed. Res. 4 (2015) 9. https://doi.org/10.4103/2277-9175.148291.

[9] M. Frydrych, S. Román, S. MacNeil, B. Chen, Biomimetic poly(glycerol sebacate)/poly(l-lactic acid) blend scaffolds for adipose tissue engineering, Acta Biomater. 18 (2015) 40–49. https://doi.org/10.1016/j.actbio.2015.03.004.

[10] J. Hu, D. Kai, H. Ye, L. Tian, X. Ding, S. Ramakrishna, X.J. Loh, Electrospinning of poly(glycerol sebacate)-based nanofibers for nerve tissue engineering, Mater. Sci. Eng. C. 70 (2017) 1089–1094. https://doi.org/10.1016/j.msec.2016.03.035.

[11] R. Rai, M. Tallawi, N. Barbani, C. Frati, D. Madeddu, S. Cavalli, G. Graiani, F. Quaini, J.A. Roether, D.W. Schubert, E. Rosellini, A.R. Boccaccini, Biomimetic poly(glycerol sebacate) (PGS) membranes for cardiac patch application, Mater. Sci. Eng. C. 33 (2013) 3677–3687. https://doi.org/10.1016/j.msec.2013.04.058.

[12] N. Masoumi, K.L. Johnson, M.C. Howell, G.C. Engelmayr, Valvular interstitial cell seeded poly(glycerol sebacate) scaffolds: Toward a biomimetic in vitro model for heart valve tissue engineering, Acta Biomater. 9 (2013) 5974–5988. https://doi.org/10.1016/j.actbio.2013.01.001.

[13] D. Lin, K. Yang, W. Tang, Y. Liu, Y. Yuan, C. Liu, A poly(glycerol sebacate)-coated mesoporous bioactive glass scaffold with adjustable mechanical strength, degradation rate, controlled-release and cell behavior for bone tissue engineering, Colloids Surfaces B Biointerfaces. 131 (2015) 1–11. https://doi.org/10.1016/j.colsurfb.2015.04.031.

[14] A. Tevlek, P. Hosseinian, C. Ogutcu, M. Turk, H.M. Aydin, Bi-layered constructs of poly(glycerol-sebacate)-β-tricalcium phosphate for bone-soft tissue interface applications, Mater. Sci. Eng. C. 72 (2017) 316–324. https://doi.org/10.1016/j.msec.2016.11.082.

[15] M. Masoudi Rad, S. Nouri Khorasani, L. Ghasemi-Mobarakeh, M.P. Prabhakaran, M.R. Foroughi, M. Kharaziha, N. Saadatkish, S. Ramakrishna, Fabrication and characterization of two-layered nanofibrous membrane for guided bone and tissue regeneration application, Mater. Sci. Eng. C. 80 (2017) 75–87. https://doi.org/10.1016/j.msec.2017.05.125.

[16] T. Hu, Y. Wu, X. Zhao, L. Wang, L. Bi, P.X. Ma, B. Guo, Micropatterned, electroactive, and biodegradable poly(glycerol sebacate)-aniline trimer elastomer for cardiac tissue engineering, Chem. Eng. J. 366 (2019) 208-222. https://doi.org/10.1016/j.cej.2019.02.072.

[17] Y. Wu, L. Wang, T. Hu, P.X. Ma, B. Guo, Conductive micropatterned polyurethane films as tissue engineering scaffolds for Schwann cells and PC12 cells, J. Colloid Interface Sci. 518 (2018) 252-262. https://doi.org/10.1016/j.cis.2018.02.036.

[18] Y. Wu, L. Wang, B. Guo, P.X. Ma, Injectable biodegradable hydrogels and microgels based on methacrylated poly(ethylene glycol)-co-poly(glycerol sebacate) multi-block copolymers: synthesis, characterization, and cell encapsulation, J. Mater. Chem. B 2 (2014) 3674-3685. https://doi.org/10.1039/c3tb21716g.

[19] M. Gultekinoglu, S. Öztürk, B. Chen, M. Edirisinghe, K. Ulubayram, Preparation of poly(glycerol sebacate) fibers for tissue engineering applications, Eur. Polym. J. 121 (2019) 109297. https://doi.org/10.1016/j.eurpolymj.2019.109297.

[20] Y. Wu, L. Wang, X. Zhao, S. Hou, B. Guo, P.X. Ma, Self-healing supramolecular bioelastomers with shape memory property as a multifunctional platform for biomedical applications via modular assembly, Biomaterials 104 (2016) 18-31. https://doi.org/10.1016/j.biomaterials.2016.07.011.

[21] X. Zhao, Y. Wu, Y. Du, X. Chen, B. Lei, Y. Xue, P.X. Ma, A highly bioactive and biodegradable poly(glycerol sebacate)-silica glass hybrid elastomer with tailored mechanical properties for none tissue regeneration, J. Mater. Chem. B 3 (2015) 3222-3233. https://doi.org/10.1039/c4tb01693a.

[22] M. Nagata, T. Machida, W. Sakai, N. Tsutsumi, Synthesis, characterization, and enzymatic degradation of network aliphatic copolyesters, J. Polym. Sci. Part A Polym.

Chem. 37 (1999) 2005–2011. https://doi.org/10.1002/(SICI)1099-0518(19990701)37:13<2005::AID-POLA14>3.0.CO;2-H.

[23] J.M. Kemppainen, S.J. Hollister, Tailoring the mechanical properties of 3D-designed poly(glycerol sebacate) scaffolds for cartilage applications, J. Biomed. Mater. Res. Part A. 94A (2010) 9–18. https://doi.org/10.1002/jbm.a.32653.

[24] Á. Conejero-García, H.R. Gimeno, Y.M. Sáez, G. Vilariño-Feltrer, I. Ortuño-Lizarán, A. Vallés-Lluch, Correlating synthesis parameters with physicochemical properties of poly(glycerol sebacate), Eur. Polym. J. 87 (2017) 406–419. https://doi.org/10.1016/j.eurpolymj.2017.01.001.

[25] R. Ravichandran, J.R. Venugopal, S. Mukherjee, S. Sundarrajan, S. Ramakrishna, Elastomeric Core/Shell Nanofibrous Cardiac Patch as a Biomimetic Support for Infarcted Porcine Myocardium, Tissue Eng. Part A. 21 (2015) 1288–1298. https://doi.org/10.1089/ten.tea.2014.0265.

[26] J. Gao, P.M. Crapo, Y. Wang, Macroporous Elastomeric Scaffolds with Extensive Micropores for Soft Tissue Engineering, Tissue Eng. 12 (2006) 917–925. https://doi.org/10.1089/ten.2006.12.917.

[27] A.G. Mitsak, A.M. Dunn, S.J. Hollister, Mechanical characterization and non-linear elastic modeling of poly(glycerol sebacate) for soft tissue engineering, J. Mech. Behav. Biomed. Mater. 11 (2012) 3–15. https://doi.org/10.1016/j.jmbbm.2011.11.003.

[28] C.-N. Hsu, P.-Y. Lee, H.-Y. Tuan-Mu, C.-Y. Li, J.-J. Hu, Fabrication of a mechanically anisotropic poly(glycerol sebacate) membrane for tissue engineering, J. Biomed. Mater. Res. Part B Appl. Biomater. 106 (2018) 760–770. https://doi.org/10.1002/jbm.b.33876.

[29] X. Li, A.T.L. Hong, N. Naskar, H.-J. Chung, Criteria for Quick and Consistent Synthesis of Poly(glycerol sebacate) for Tailored Mechanical Properties, Biomacromolecules. 16 (2015) 1525–1533. https://doi.org/10.1021/acs.biomac.5b00018.

[30] H.M. Aydin, K. Salimi, Z.M.O. Rzayev, E. Pişkin, Microwave-assisted rapid synthesis of poly(glycerol-sebacate) elastomers, Biomater. Sci. 1 (2013) 503–509. https://doi.org/10.1039/c3bm00157a.

[31] C.C. Lau, M.K. Bayazit, J.C. Knowles, J. Tang, Tailoring degree of esterification and branching of poly(glycerol sebacate) by energy efficient microwave irradiation, Polym. Chem. 8 (2017) 3937–3947. https://doi.org/10.1039/c7py00862g.

[32] V.A. Bhanu, K. Kishore, Role of oxygen in polymerization reactions, Chem. Rev. 91 (1991) 99–117. https://doi.org/10.1021/cr00002a001.

[33] R.T. Conley, Studies of the Stability of Condensation Polymers in Oxygen-Containing Atmospheres, J. Macromol. Sci. Part A - Chem. 1 (1967) 81–106. https://doi.org/10.1080/10601326708053918.

[34] J. Langer, Chemical Properties and Derivatives of Glycerol, Ann. Phys. (N. Y). (1969). https://www.aciscience.org/docs/Chemical_Properties_and_Derivatives_of_Glycerol.pdf.

[35] M. SZWARC, 'Living' Polymers, Nature. 178 (1956) 1168–1169. https://doi.org/10.1038/1781168a0.

[36] Q.-Z. Chen, A. Bismarck, U. Hansen, S. Junaid, M.Q. Tran, S.E. Harding, N.N. Ali, A.R. Boccaccini, Characterisation of a soft elastomer poly(glycerol sebacate) designed to match the mechanical properties of myocardial tissue, Biomaterials. 29 (2008) 47–57. https://doi.org/10.1016/j.biomaterials.2007.09.010.

[37] A. Vallés-Lluch, G. Gallego Ferrer, M. Monleón Pradas, Effect of the silica content on the physico-chemical and relaxation properties of hybrid polymer/silica nanocomposites of P(EMA-co-HEA), Eur. Polym. J. 46 (2010) 910–917. https://doi.org/10.1016/j.eurpolymj.2010.02.004.

[38] A.K. Gaharwar, A. Patel, A. Dolatshahi-Pirouz, H. Zhang, K. Rangarajan, G. Iviglia, S.-R. Shin, M.A. Hussain, A. Khademhosseini, Elastomeric nanocomposite scaffolds made from poly(glycerol sebacate) chemically crosslinked with carbon nanotubes, Biomater. Sci. 3 (2015) 46–58. https://doi.org/10.1039/C4BM00222A.

[39] Q. Chen, S. Liang, G.A. Thouas, Elastomeric biomaterials for tissue engineering, Progress in Polymer Science 38 (2013) 584– 671. http://dx.doi.org/10.1016/j.progpolymsci.2012.05.003.

[40] Y. Ma, X. Feng, J.A. Rogers, Y. Huang, Y. Zhang, Design and application of 'J-shaped' stress-strain behavior in stretchable electronics: a review, Lab Chip. 17(10) (2017): 1689–1704. https://www.doi.org/10.1039/c7lc00289k.

[41] R. Maliger, P.J. Halley, J.J. Cooper-White, Poly(glycerol-sebacate) bioleastomers-kinetics of step-growth reactions using Fourier Transform (FT)-Raman spectroscopy, J. Appl. Polym Sci. (2012) 1-7. https://www.doi.org/10.1002/app.37719.

[42] J.L. Ifkovits, R.F. Padera, J.A. Burdick, Biodegradable and radically polymerized elastomers with enhanced processing capabilities, Biomed Mater. 3 (2008) 034104 (8pp). https://www.doi.org/10.1088/1748-6041/3/3/034104.